A pulsed microchannel-plate-based non-neutral plasma imaging system

A. J. Peurrung and J. Fajans
Department of Physics, University of California, Berkeley, Berkeley, California 94720

(Received 23 June 1992; accepted for publication 21 September 1992)

The design and operation of a pure electron plasma imaging system is described. The system yields images with high resolution and a large dynamic range. A two-dimensional image of the plasma is acquired by streaming the plasma directly onto a microchannel plate and phosphor screen. Resolution of the rapidly evolving plasma requires that all the plasma strike the microchannel plate in a single charge pulse lasting less than 1 μs. The expected performance and actual operational characteristics of the system are detailed, with special attention given to the properties of a microchannel plate used in a pulsed imaging mode.

I. INTRODUCTION

We have designed and operated a pulsed, microchannel-plate-based system for single-shot imaging of a pure electron plasma. Although the diagnostic destroys the imaged plasma, it yields a complete, line-integrated, two-dimensional profile from each plasma. This imaging capability has proved to be invaluable in our study of the dynamics of pure electron plasmas.[1–3] A similar diagnostic could successfully image any type of non-neutral plasma composed of particles detectable by microchannel plates.[4] Figure 1 shows two typical pure electron plasma images.

The formation of pulsed images requires that our microchannel plate must be used in a novel operational mode. Normally, a microchannel plate (hereafter MCP) is used in one of two distinct modes. In the "analog" mode, used in applications such as image intensifiers and electron beam diagnostics, the MCP amplifies a continuous, low-intensity stream of electrons or other particles.[5] In this mode, the MCP is not saturated, and it yields quantitative information about the spatial distribution and intensity of the incoming particles. In the "pulse current" mode, the MCP is used to detect individual particles. The arrival time and spatial location of each particle is easily determined as each particle produces a large, saturated, output pulse. Our application involves pulsed imaging across the entire MCP at once. Thus we combine the analog nature of the first operational mode with the pulsed nature of the second. By boosting the amount of available charge, the MCP increases the dynamic range, while preserving the high resolution of our image. Unfortunately, image linearity is lost because the output of the MCP is partially saturated.

Our plasma imaging system is related to various devices which permit optical imaging with low light levels. The combination of photocathode, MCP, and phosphor has long been used for image amplification in various widely available image intensifier tubes. Several image intensifiers have employed fiber optic elements to reduce the image size and transmit the image to a charge-coupled device (CCD) camera.[6,7] In our device the pure electron plasma replaces the proximity focused photocathode as the electron source. Since in our machine proximity focusing cannot be used to prevent image blurring, we carefully suppress plasma drifts which might occur during the acceleration of the plasma toward the MCP.

Previous pure electron plasma imaging techniques have used single-point charge collectors to assemble images pixel by pixel. The collector is movable along one line only; acquisition of two-dimensional images relies on synchronized plasma rotation.[8] Although useful in many situations, this system has several disadvantages. Since thousands of plasmas must often be created and destroyed for a single image, image acquisition is quite time consuming. In addition, if the plasma rotational phase cannot be accurately controlled, then two-dimensional images will be difficult or impossible to acquire. This problem arises if the plasma is externally symmetric, or if the plasma is in a stationary, noncircular equilibrium.[1] Finally, only a single-shot imaging system can image turbulent or unpredictable plasma dynamics. Unless the dynamical state is recreated exactly, noise will hide much of the interesting behavior.

II. SYSTEM DESIGN

Figure 2 shows a schematic of the imaging system. An image is produced when the plasma electrons are dumped onto a MCP of thickness 0.53 mm, channel diameter 12 μm, and active diameter 4.2 cm.[9] This diameter is larger than that of our largest plasmas (3.8 cm). The MCP is capable of producing gains of 10^4 but is normally run with effective gains of less than 10^3. The electrons produced by the MCP are accelerated to an energy of approximately 5 keV and sent into a phosphor screen. We chose P20 phosphor for its high light generation efficiency and because it produces light at a wavelength easily transmitted by fiber optics and detected by CCD cameras. The MCP and the phosphor screen operate in an ultrahigh vacuum ($\sim 10^{-11}$ Torr).

Image preserving fiber optic elements are used to evenly and efficiently carry the optical image to the CCD camera. The phosphor screen is deposited on a solid fiber optic faceplate which also serves as a vacuum window. The image is reduced in size by a 5 to 1 demagnifying taper and then enters a 36-in.-long, flexible, fiber optic cable. The cable leads to an external camera which has a fiber optic plate glued directly to a thermoelectrically cooled, 8.8 $\times$ 11.4-mm CCD array. All fiber optic elements are joined

 0034-6748/93/010052-04$06.00

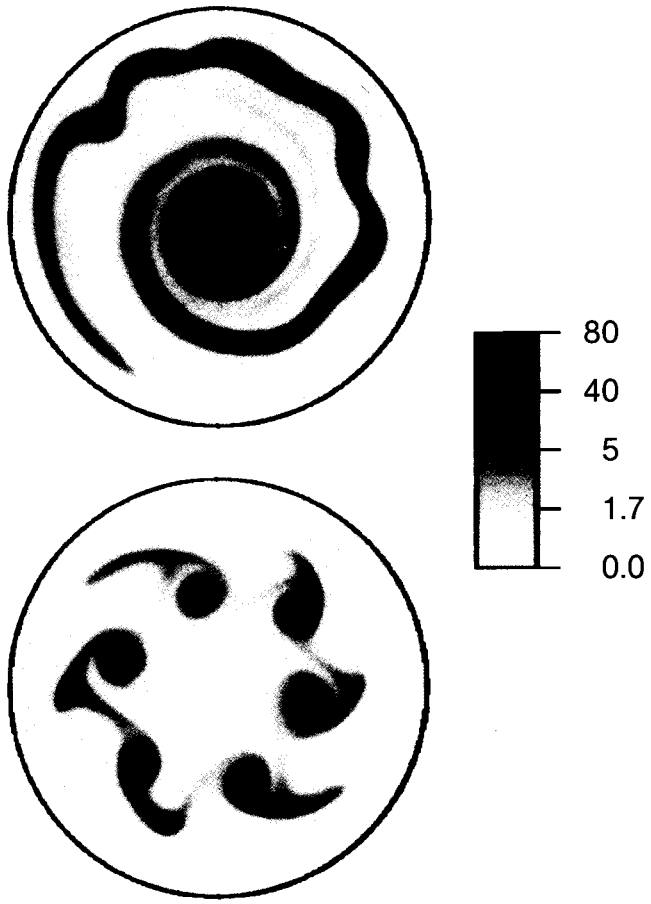

FIG. 1. Sample images of a pure electron plasma. The unit of density is 10^7 cm^{-2}. The outer circle indicates the outer confining wall.

using diffusion pump oil to match the index of refraction. Unlike other oils, diffusion pump oil does not evaporate at the high temperatures reached during the vacuum bakeout. We avoid vacuum outgassing problems by placing all the fiber optic elements (except for the phosphor faceplate) outside the ultrahigh vacuum region. Electrons leaving the plasma confinement region at the start of the imaging process have energies from 1 to 50 eV. The MCP operates most efficiently when the incident electrons have energies

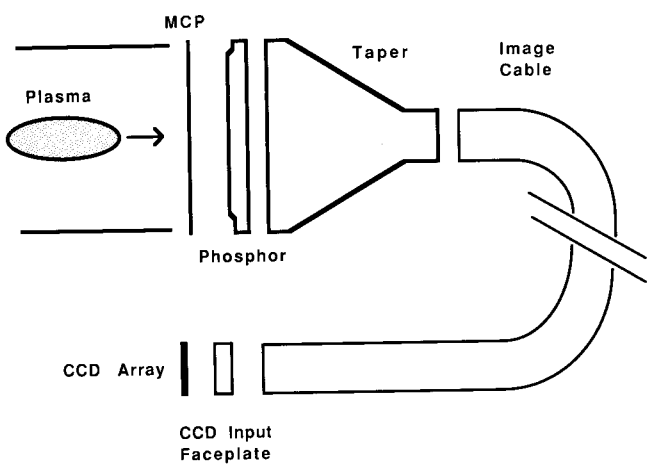

FIG. 2. System schematic.

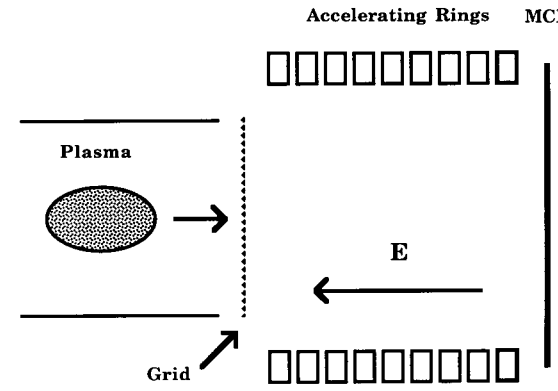

FIG. 3. Side view section of the acceleration region.

above 300 eV. We must therefore accelerate the electrons before they strike the MCP. If not carefully undertaken, this acceleration can be a source of image distortion. The desired accelerating electric field, E_z, is directed axially and is not, of course, detrimental. However, any radial electric fields E_r cause azimuthal drifts with a velocity $v \propto E_r/B$, where B is the axial magnetic field. A particle of mass m and charge q transits the acceleration region in a time $\tau \propto \sqrt{m/qE_z}$. Thus

$$L \propto \frac{E_r}{B}\sqrt{\frac{m}{qE_z}},$$

where L measures the distortion. For a given acceleration geometry both E_r and E_z are proportional to the acceleration voltage V. Consequently,

$$L \propto \sqrt{\frac{mV}{qB^2}}.$$

Thus the distortion is proportional to the square root of the acceleration voltage. Typically, a phosphor screen operated alone requires an acceleration voltage of 10 kV. We therefore obtain a sevenfold improvement in image distortion by operating the MCP at an acceleration voltage of 200 V.

Despite the low acceleration voltages, our images are still subject to significant distortion at low magnetic fields. This distortion is reduced by minimizing the radial electric fields. Figure 3 details the construction of our acceleration region. The nine carefully biased acceleration rings and the grounded grid insure nearly axial electric fields. The grid, made from 25-μm tungsten wire, absorbs no more than 1% of passing electrons. The grid also prevents penetration of the imaging system electric fields into the plasma confinement region.

III. OPERATION

This section describes the operation of the imaging system and the performance of the MCP and other system elements.

A. Image brightness

For our application it is the maximum MCP output charge, instead of MCP gain, that limits image brightness.

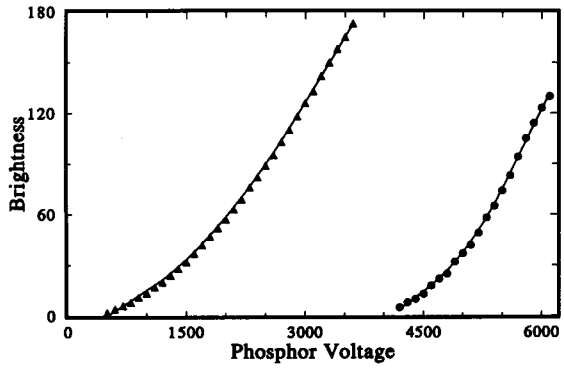

FIG. 4. Image brightness vs phosphor voltage. Circular symbols represent the aluminized phosphor screen; triangles represent the nonaluminized phosphor. The unit of brightness is arbitrary.

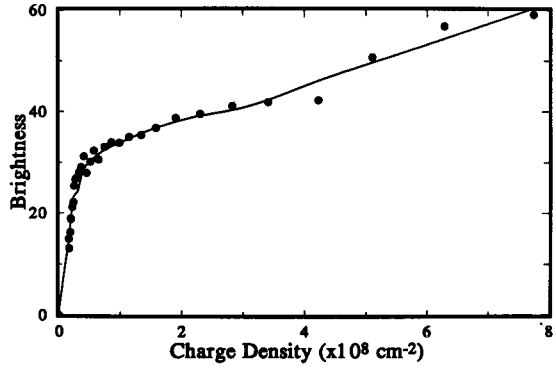

FIG. 5. Image brightness vs input charge density. The unit of brightness is arbitrary.

The instantaneous removal of more than 1 nC/cm^2 begins to cause saturation of the MCP.[10,11] Since a typical plasma has a charge density of 10^8 e^-/cm^2 (1.6×10^{-11} C/cm^2), the MCP will begin to saturate above a gain of 10^2. Increasing the gain above this value does not result in substantially brighter images, and does introduce nonlinearities.

The primary factor which affects image brightness is the energy of the electrons striking the phosphor screen. Figure 4 shows image brightness as a function of phosphor screen acceleration voltage for two different types of phosphor screens. We have used both uncoated and aluminized phosphor screens in our imaging system. Although it gives less light, the aluminized phosphor is more rugged and blocks unwanted visible photons produced elsewhere in the system. Full white in our camera corresponds to an integrated flux of 2×10^{11} photons/cm^2. Assuming a fiber optic transmission efficiency of 25%, we calculate that at 5000 V the aluminized phosphor screen yields 130 useful photons for every incident electron.

B. Image quality

The 400×400 pixel CCD array usually limits the image resolution. Under some conditions, particularly at low magnetic fields, azimuthal drifts in the acceleration region may limit the effective resolution. Image noise arises from the coupling of system elements with different fiber or channel spacings. For example, since the phosphor screen fiber optic faceplate has 10-μm fibers but the adjoining taper has 15-μm fibers, adjacent taper fibers may receive different amounts of light. Although the magnitude of this type of noise is approximately 10%, it is entirely repeatable and can be eliminated by correcting for the known noise pattern.

The MCP contains at least six million channels in the image area. There are shot-to-shot input level fluctuations of approximately 8% per channel because a typical plasma contains only 150 electrons for every MCP channel. Since the output pulse height for a single incident electron varies considerably,[12] we expect uncorrelated output fluctuations which may also approach the 8% level. The total output fluctuation level is therefore approximately 11% per channel. However, since approximately 70 MCP channels contribute to each camera pixel, these fluctuations are considerably reduced. Typically, we observe shot-to-shot noise levels of less than 2%, and much of this may be due to external effects such as plasma nonreproducibility.

C. Linearity

We operate the MCP near saturation in order to achieve satisfactory image brightness. Figure 5 shows the nonlinear dependence of image brightness on input charge density. The expected gain with 800 V across the MCP is 10^3, but only the linear, lower part of Fig. 5 yields this value. Although some sensitivity is lost for higher charge densities, our measured brightness can be linearized by deconvolution. Unfortunately, each MCP operating voltage requires a separate calibration. The partial saturation of the MCP output also affects the relationship between image brightness and incident electron energy. As shown in Fig. 6, when operated near saturation, the MCP is relatively insensitive to the incident electron energy. Although single electron detection efficiency drops substantially at low energy,[4] the decline in our output level is less than a factor of 2. Since the plasma contains approximately 150 electrons per channel, fewer electrons are detected, but these electrons will produce larger output cascades.

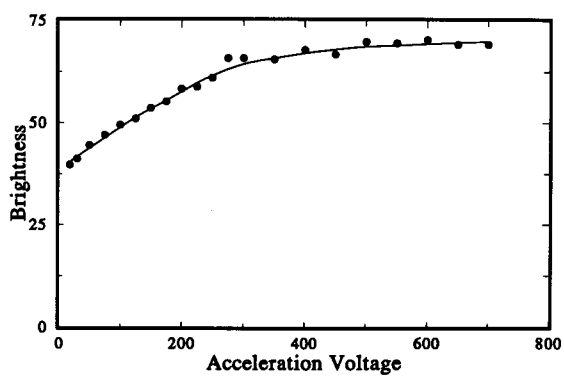

FIG. 6. Image brightness vs the acceleration voltage for electrons incident on the MCP. The unit of brightness is arbitrary.

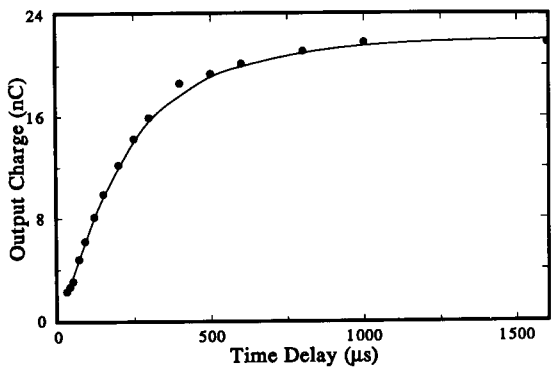

FIG. 7. MCP output charge from the second of two identical plasmas vs the time interval.

D. Speed

The entire plasma strikes the MCP within 1 μs of the opening of the trap. Since the transit time across the MCP is less than 1 ns,[11] the MCP delivers its charge to the phosphor screen without delay. Once excited, the phosphor emits light with a decay time on the order of 100 μs. The camera is therefore set to record these "flash" events and immediately begins transferring its data to computer storage. Reading the image from the CCD array requires approximately 150 ms. The overall speed of the imaging system is seldom a problem since plasma formation and manipulation usually take much longer.

After a plasma strikes the MCP, some time is required before the MCP recovers.[10–12] During this "dead time," the MCP exhibits a lower effective gain than normal. This effect would limit the image acquisition speed if a faster camera were used or if only one plasma from a rapid sequence is imaged. We determine the MCP recovery time by measuring the MCP output charge from two identical plasmas separated by a variable time delay. Figure 7 plots the brightness of the second image as a function of the delay interval. Under these conditions the MCP recovers almost completely in 1 ms. This rapid recovery time results from the low electrical resistance (3 MΩ) of Galileo's high output technology ("HOT") MCPs.[10–12]

ACKNOWLEDGMENTS

This work is supported by the ONR and the LLNL PPRI.

[1] J. Notte, A. J. Peurrung, J. Fajans, R. Chu, and J. S. Wurtele (submitted).
[2] A. J. Peurrung and J. Fajans, Phys. Fluids A (to be published).
[3] A. J. Peurrung, J. Notte, and J. Fajans (submitted).
[4] J. P. Macau, J. Jamar, and S. Gardier, IEEE Trans. Nucl. Sci. **NS-23**, 2049 (1976).
[5] C. A. Timmer, Ph.D. thesis, University of Colorado, Boulder, CO (1988).
[6] M. K. Carter, B. E. Brachett, P. D. Reed, and N. Walthan, Nucl. Instrum. Methods Phys. Res. A **310**, 305 (1991).
[7] J. L. A. Fordham, J. G. Bellis, D. A. Bone, and T. J . Norton, Proc. SPIE **1449**, 87 (1991).
[8] C. F. Driscoll, J. H. Malmberg, K. S. Fine, R. A. Smith, X.-P. Huang, and R. W. Gould, in *Plasma Physics and Controlled Nuclear Fusion Research 1988* (IAEA, Vienna, 1989), Vol. 3, pp. 507–514.
[9] A high output technology microchannel plate (part No. 1330-3360) manufactured by Galileo Electro-Optics Corporation was used for all of these experiments.
[10] C. Loty, Acto Electronica **14**, 107 (1971).
[11] E. H. Eberhardt, IEEE Trans. Nucl. Sci. **NS-28**, 712 (1981).
[12] J. L. Wiza, Nucl. Instrum. Methods **162**, 587 (1979).